Improving the performance of neural network using wavelet transformation on dynamic MR imaging

Parviz Abdolmaleki[1], Ph.D., Hamid Abrishami moghddam[2], Ph.D, Masomeh Gitee[3],M.D, Abbas Mostafa[2], Ms.c

[1.]Department of Biophysics , Tarbiat Modares University

e-mail: parviz@modares.ac.ir

Abstracts: In an attempt to differentiate malignant from benign in a group of patients with histopathologically proved breast lesions based on the data derived independently from time-intensity curve using the wavelet transform an neural network established.The performance of ANN was evaluated using a database with 105 patients' records each of which consisted of 8 quantitative parameters mostly derived from time-intensity curve using wavelet transform. These findings were encoded as features for a three-layered neural network to predict the outcome of biopsy. The network was trained and tested using the jackknife method and its performance was then compared to that of the radiologists in terms of sensitivity, specificity and accuracy using receiver operating characteristic curve (ROC) analysis.The network was able to classify correctly of 84 original cases and yielded a comparable diagnostic accuracy (80%), compared to that of the radiologist (85%) by performing a constructive association between extracted quantitative data and corresponding pathological results ($r=0.63$, $p<0.001$) . An ANN supported by wavelet transform can be trained to differentiate malignant from benign with a reasonable degree of accuracy.

Keywords: wavelet transform, neural network, and ROC curve.

1. Introduction

In the clinical setting, the ANN has been widely applied in breast cancer diagnosis using subjective impression of different features based on defined criteria [1,2]. Although it is widely showed good performance but some report has shown some disadvantages such as; the presence of the inter and intraobserver disagreement in features categorization as well as final interpretation [3]. This variability causes an inconsistency in feature categorization as well as final diagnosis. Using such subjective data which strongly relies on the correctness of observer interpretation as input into the ANN sometimes make a confuseable situation for ANN and therefore affect the performance of neural network [3]. Recently some reports suggested the possibility of using directly extracted quantitative features as input into the ANN in a few fields of radiology in which the quantitative data is accessible [3].In this study we developed a computerized method to extract quantitative features directly from computer generated time-intensity curves using wavelet transform and analyzing them using an ANN. Our objectives in this study were (1) To extract independent featuers directly from time-intensity porofile using wavelet transform,

(2) To minimize the reliance of the output of the ANN on the correctness of radiological interpretation which it is depend to the factors like the experience of the reader, time of reading and criteria used for extracting the data.

2. Methods

We employed a three-layered, feedforward neural network with a back propagation algorithm for training. The network designed to distinguish benign and malignant on the basis of features that had been extracted from signal-intensity profile using wavelet transform. Our study group consisted of 104 female patients whose ages ranged from 15 to 79 years (mean 52 yrs). The patients group included 75 malignant lesions and 30 benign entities. All patients underwent excisional biopsy (n= 105).

2.1 Wavelet Transform

The wavelet transform can be regarded as a signal expansion using a set of basis functions, which are obtained from a single prototype function $\psi(x)$, called *Mother Wavelet*. By definition a function $\psi(x)$ can be considered to be mother wavelet if [10]

$$\int_{-\infty}^{\infty} \psi(x)dx = \Psi(0) = 0$$

where $\Psi(\omega)$ is the Fourier transform of the function $\psi(x)$. The wavelet transform of a 1D real function $f(x) \in L^2(R)$ with respect to a mother wavelet $\psi(x)$ is defined as

$$W(s,t) = \frac{1}{\sqrt{|s|}} \int_{-\infty}^{\infty} f(x)\psi(\frac{x-t}{s})dx$$

The wavelet transform $W(s,t)$ gives a scale-space decomposition of the signal $f(x)$ with s indexing the scale and t indexing position in the original signal space. In practice, the wavelet transform scale and translation parameters are discretized and for fast numerical implementation the scale normally varies along a dyadic sequence. This yields the *Discrete Dyadic Wavelet Transform*:

$$W(j,n) = 2^{-j/2} \int_{-\infty}^{\infty} f(x)\psi(2^{-j}(x-n))dx$$

For a discrete signal of length N, the maximum number of available scales is defined as $J = \log_2(n) + 1$. Figure (1) shows wavelet decompositions in two levels using Daubechies wavelets. In figure (1.a), wavelet coefficients corresponding to a benign case signal is illustrated. Wavelet decomposition of a malignant case signal is shown in figure (1.b). In this figures no subsampling has been applied.

2.2 Data acquisition

2.2.1 MR imaging: MR imaging was performed using a Signa 1.5 Tesla unit (GE Medical Systems, Milwaukee, Wis) in the prone position with a single 5-inch circular general-purpose surface coil. Initial sagittal or axial T1-weighted spin-echo images (T1W) were performed at 400/16 (repetition time msec/ echo time msec) and axial or sagittal T2-weighted fast spin-echo images (T2W) were performed at 3,000/108. Other MR parameters used were 22 cm field of view, 3.6 mm section thickness, and 256×192 (T1-weighted) or 256 × 256 (T2-weighted) matrix. Dynamic study was performed after administration of gadopentetate dimeglumine (Magnevist; Schering, Berlin, Germany) over 10-15 seconds using a fast radio-frequency spoiled gradient-recalled-echo (SPGR) sequence (11.4/3.3; flip angle,10 degree; matrix, 256 ×192; section thickness, 3.6 mm; gap, 1.0-2.5 mm).

2.2.2 Feature Generation:

For the quantitative assessment **t**he images were called back one by one and a free size ROI were drawn in the most enhancing part of the lesion (figure 2).

The obtained time-intensity values were used to generate the time intensity curve. A locally written program based on wavelet analysis was then used to obtain

the following features from the signal intensity profile:

1) The variance of the high frequency coefficients in the first scale of wavelet transform for the 5 early points of the signal in wash-in part of the signal intensity curve.
2) The variance of the high frequency coefficients in the second scale of wavelet transform for the 4 early points of the signal in wash-in part of the signal intensity curve.
3) The variance of the high frequency coefficients in the first scale of wavelet transform for the 6 last points of the signal in wash-out part of the signal intensity curve.
4) The variance of the high frequency coefficients in the second scale of wavelet transform for the 4 last points of the signal in wash-out part of the signal intensity curve.
5) The variance of the low frequency coefficients in the first scale of wavelet transform for the 6 last points of the signal in wash-out part of the signal intensity curve.
6) The variance of the low frequency coefficients in the second scale of wavelet transform for the 4 last points of the signal in wash-out part of the signal intensity curve
7) The energy of the high frequency coefficients in the first scale of wavelet transform for the whole signal.
8) The energy of the high frequency coefficients in the second scale of wavelet transform for the whole signal.

These eight features were selected on the basis of their qualitative correlation with medical experience. Table 1 shows the parameters in our database, which represented all extracted features from the analyzing the signal-intensity profile using wavelet transformation. For the simulation of the neural network, all the quantitative data were normalized between 0 and 1 according to the maximum value of each feature in the data set. The normalized data was then fedforward into the network to map them with corresponding pathological findings.

2.2.3 Radiological assessment: One reader (MG) was then asked to read and report their findings from conventional pre and post contract T1 and T2-weighted images as well as dynamic images. Imaging findings were graded on the following features; size, shape, lesion margin, enhancement homogeneity, time-intensity curve type, as well as other associated features. The classification for the curve type has been previously reported [5].

2.2.4 Neural networks structure: The neural network, which was employed in this study had three layers. The first layer consisted of 8 input elements, each of which corresponded to data extracted from the wavelet analysis on signal intensity profile; the second layer, the hidden layer, had 5 nodes and finally the output layer with 1 elements, which represented 1 for malignant and 0 for benign lesions. In order to determine the best optimized structure for the neural network, we simulated a large number of neural networks by varying the number of hidden nodes, iterations and learning rates.

Our network was trained and tested using the jackknife technique in which all cases were used in both the training and testing processes [6]. In this method, all but one case in the database is used to train the network. The single case that is left out is then used to test the network. This procedure is repeated until each case in the database is used once as a testing case.

Finally, after the network had been trained perfectly in each simulation the testing case was presented to the trained network giving a diagnostic output vector in the range of (0-1). Our network was trained perfectly over 200,000 iterations on a IBM compatible personal computer (Pentium III 800 MHz). The software used to construct the neural network was written

locally in MATLAB programming language [7].

2.3 Performance Evaluation:

The sophisticated ROC analysis was chosen to evaluate the performance of neural network approach and that of radiologists [8]. After the network had been trained perfectly in each simulation the testing set was presented to the trained network giving a diagnostic output vector in the range of (0-1). The outputs of the testing set were then analyzed to determine the true-positive and the false-positive fractions, which were then used for plotting the ROC curves. The area under the ROC curve (A_z) was then used to compare the performance of ANN as well as the radiologist participating in the testing procedure.

To evaluate the performance of the observers, an expert reader (MG) was asked to record their findings into one of the five categories with increasing likelihood of malignancy; 1= benign, 2= probably benign, 3= indeterminate, 4= probably malignant, 5= malignant. Similarly, to evaluate the performance of the neural network, the network output was classified into five categories; output in range of (0-0.2)= benign, (0.2- 0.4)= probably benign, (0.4-0.6)=equivocal, (0.6-0.8)= probably malignant and output in range of (0.8-1)= malignant.

3. RESULTS

3.1 Radiologist performance: One expert reviewer with high level of experience read the images and classified them into benign and malignant groups using a five-scale category with increasing likelihood of malignancy. The average output for reader was a sensitivity of 91%, specificity of 70%, and an accuracy of 85%.

3.2 Neural network performance: We applied the conventional jackknife method to the training database of 105 cases. The output of neural network showed a correct classification for 65 of 75 of the patients with malignant breast cancers and 19 of 30 with benign entity. This yielded a diagnostic accuracy (80%) for the ANN, which is comparable to the average outcomes obtained for the high experienced radiologists (85%). Table 2 summarizes the average results obtained for the participating radiologist compared with the prediction of neural network in terms of sensitivity, specificity, accuracy, false positive, false negative, misclassified rate. Figure 3 demonstrate a comparative histogram of the evaluated performance for the Artificial Neural Network and the participated radiologist.

we also applied ROC analysis to our data to confirm the results obtained. Using the best results obtained for the radiologist as well as the ANN an ROC analysis was performed. The area under the receiver operating characteristic curves (Az) for the ANN was Az (net) = 0.8625 ± 0.0561, with an accuracy of 80%, for the participated radiologist Az(doc) = 0.9265 ± 0.0088, with a maximum of 85% accuracy.

4. Discussion:

In this study we assumed that applying the quantitative parameters extracted using wavelet transform and analyzed by an ANN program can possibly reduce the present overlap between the benign and malignant patterns. This assumption is justified by the wavelet transform ability to separate frequency components of the signal and represent them as a function of time. In other words, wavelet transform of the signal intensity profile is a 2D map representing frequency components of the signal in different time intervals. This can somehow explain the phase of the trace of contrast medium in wash-in and wash-out part of bolus injection. To achieve this purpose, we analyzed the temporal

progression of contrast enhancement by plotting the rate of change of signal intensity as a function of time. In addition, we analyzed the time intensity curves basing it on the peak enhancement and wash-out of the contrast medium. In this regard the two first parameters which somehow represent the gradient of the steepest part of the contrast uptake curve were then included. Because it is reported that the presence of the sharp enhancement especially during the early phase (within 120 seconds after the bolus injection) has a strong correlation with the histopathologic findings. Also the features 3 to 6 were included because they represent the change of the contrast enhancement in the wash-out part of signal intensity curve. Moreover, features 7 and 8 are used to represent overall distortions of the measured signals. These features can have a normalization effect on the other 6 features. That means if a defined signal is very oscillating, its energy features (7,8) will be larger and the gradient measures in features 1 to 6 will be normalized by these larger energy values. Among the too many available independent quantitative parameters we selected those with some similarities with the contrast enhancement as input into the ANN. The previous reports suggested the great power of the ANN in making association between too many independent linear and/or nonlinear parameters. This happened by establishing similarities between evaluated parameters in the training set during the training process by addressing them as proportional weights. These defined weights was then used during the testing process to evaluate the degree of malignancy for the cases that have not been previously presented to the computer. In this regard we applied our program to a population of patients with proven histopathological findings to predict the outcome of biopsy based on the quantitative data extracted directly from signal intensity profile using wavelet transform.

Using such objective quantitative data our network was trained and tested by the conventional round rubbin method on 105 proven cases. Our goals were to reduce the number of benign cases sent to biopsy using neural network as a supportive tool based on data extracted from time intensity curves using wavelet transform. By doing so, we eliminate the reliance of the output of the ANN on the correctness of radiological interpretation which it is depend to the factors like the experience of the reader, time of reading and criteria used for extracting the data. The overall average results for sensitivity, specificity, and accuracy of 87%, 63%, and 80% for the ANN were comparable with those obtained for participated expert ardiologist: 91%, 70%, and 85%. This indicates that a three-layer feed-forward neural network jointed with a preprocessor in the form of wavelet transform can be trained to successfully support radiologists in differentiating malignant from benign breast tumors. The moderate obtained of the low specificity may prove the previous report suggesting that the apparent overlap may be due to a inherent biological overlap [9].

5. References

1.Hollingsworth AB, Stough RG.The emerging role of breast magnetic resonance imaging. J Okla State Med Assoc. 2003 Jul;96(7):299-307. Review.

2.Peek ME. Screening mammography in the elderly: a review of the issues. J Am Med Womens Assoc. 2003 Summer;58(3):191-8.

3.Elmore JG, Nakano CY, Koepsell TD, et al. International variation in screening mammography interpretations in community-based programs. J Natl Cancer Inst. 2003 Sep 17; 95(18):1384-93.

4.Mallat SG, A wavelet tour of signal processing, Academic Press, 2nd Edition, 1999.

5.Buadu-LD; Murakami-J; Murayama-S; et al. Breast lesions: correlation of contrast medium enhancement patterns on MR images with histopathologic findings and tumor angiogenesis. Radiology. 1996 Sep; 200(3): 639-49

6.Tourassi GD. Floyd CE Sostman HD, Coleman RE. An artificial neural network approach for the diagnosis of acute pulmonary embolism. Radiology 1993;189:555-8.

7.MATLAB user's guide. The Math Works Inc., 2002.

8.Metz CE. Some practical issues of experimental design and data analysis in radiological ROC studies. Invest Radiol, 24: 234-245,1989

9. Ivanovic V, Todorovic-Rakovic N, Demajo M, et al. Elevated plasma levels of transforming growth factor-beta 1 (TGF-beta 1) in patients with advanced breast cancer: association with disease progression. Eur J Cancer. 2003 Mar;39(4):454-61.

Table 1: The extracted quantitative parameters from time-intensity profile which used as input into the neural network.

Indexes	Mean ± S.D. 1.0e+003 *	Range 1.0e+003 *
1. The VHFC* in the first scale of WT** for the 5 early points of the signal in wash-in part of the SI*** curve.	0.1648 ± 0.2393	1.260
2. The VHFC in the second scale of WT for the 4 early points of the signal in wash-in part of the SI curve.	1.0459±1.3422	7.327
3. The VHFC in the first scale of WT for for the 6 last points of the signal in wash-out part of the SI curve.	0.0267± 0.0475	0.3350
4. The VHFC in the second scale of WT for the 4 last points of the signal in wash-out part of the SI curve.	0.0219 ± 0.0361	0.1990
5. The VLFC**** in the first scale of WT for the 6 last points of the signal in wash-out part of the SI curve.	0.0269 ± 0.0455	0.2630
6. The VLFC in the second scale of WT for the 4 last points of the signal in wash-out part of the SI curve	0.0296 ± 0.0627	0.4260
7. The energy of the high frequency coefficients in the first scale of WT for the whole signal.	0.9414 ± 1.2410	6.6620
8. The energy of the high frequency coefficients in the second scale of WT for the whole signal.	3.4182 ± 4.4968	27.7740

Note: * Variance of the high frequency coefficients in the first scale ** Wavelet transformation
*** Signal intensity **** Variance of the coefficient of the low frequency

Table 2. Comparative performance of ANN and participating radiologists.

Parameter	Participating expert radiologist	Artificial neural network
Sensitivity (%)	91	87
Specificity (%)	70	63
Accuracy (%)	85	80
False positive fraction	9 of 30	11 of 30
False negative fraction	7 of 75	10 of 75
No. of cases with no diagnosis	16	21
Misclassified rate (%)	15	20

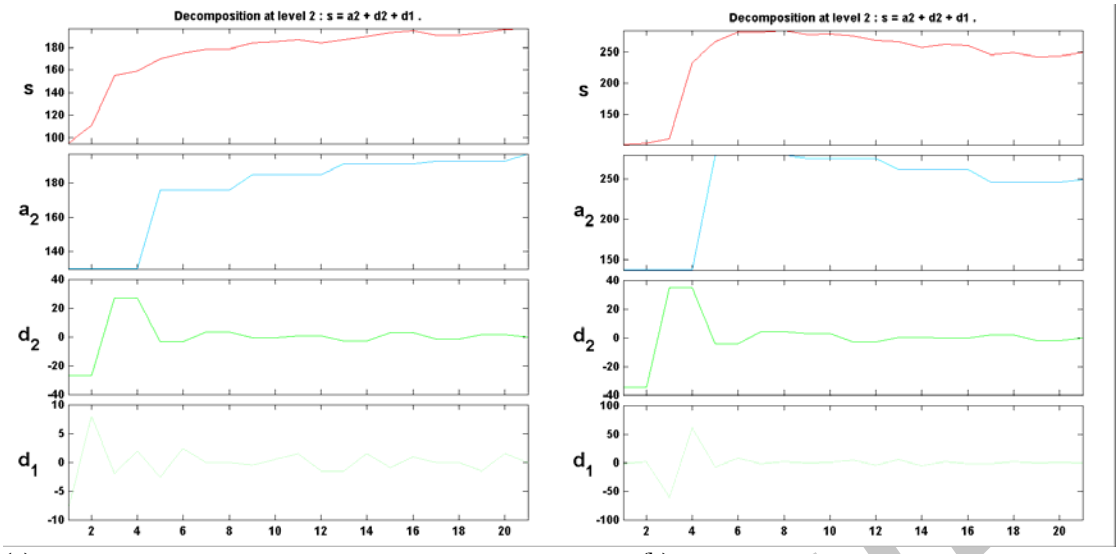

(a) (b)

Figure 1. Two level wavelet decomposition using Daubechies wavelets of (a) benign and (b) malignant signals. No subsampling has been applied.

Figure 2. Free size ROI were drawn in the most enhancing part of the lesion.

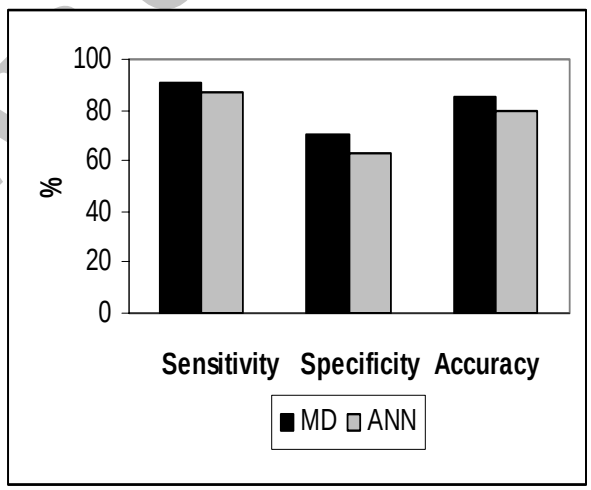

Figure 3: Comparative histogram showing average accuracy, sensitivity, and specificity of the participating radiologist and neural network